Elsevier Editorial System(tm) for Materials Science & Engineering A
Manuscript Draft

Manuscript Number:

Title: Room temperature nanoindentation creep of hot-pressed B6O

Article Type: Research Paper

Keywords: B6O; boron suboxide; nanoindentation; nanoindentation creep; nano-mechanical properties

Corresponding Author: Dr. Ronald Machaka, Ph.D.

Corresponding Author's Institution: Council for Scientific and Industrial Research

First Author: Ronald Machaka, Ph.D.

Order of Authors: Ronald Machaka, Ph.D.; Trevor E Derry, PhD; Iakovos Sigalas, PhD

Abstract: Nanoindentation has become a widely-used and versatile means of characterizing the near-surface nano-mechanical properties of a wide variety of materials. Yet, the nano-mechanical properties of polycrystalline boron suboxide material prepared by uniaxial hot-pressing are sparsely known. We recently reported on the nanoindentation profiles, nanoindentation hardness, and elastic modulus determined by using the Oliver-Pharr method. To complement our earlier reports on the analysis of the load-displacement indentation response of hot-pressed B6O and for the first time, we present and discuss results giving an insight into the temporal evolution of the nanoindentation creep behavior in B6O ceramics.

Room temperature nanoindentation creep of hot-pressed B_6O

Ronald Machaka[a,b,*], Trevor E. Derry[b,d], Iakovos Sigalas[b,c]

[a]*Light Metals, Materials Science and Manufacturing, Council for Scientific and Industrial Research, P.O. Box 395, Pretoria 0001, South Africa*

[b]*DST/NRF Centre of Excellence in Strong Materials, University of the Witwatersrand, Private Bag 3, Wits, Johannesburg 2050, South Africa*

[c]*School of Chemical and Metallurgical Engineering, University of the Witwatersrand, Private Bag 3, Wits, Johannesburg 2050, South Africa*

[d]*School of Physics, University of the Witwatersrand, Private Bag 3, Wits, Johannesburg 2050, 2050 South Africa*

Abstract: Nanoindentation has become a widely-used and versatile means of characterizing the near-surface nano-mechanical properties of a wide variety of materials. Yet, the nano-mechanical properties of polycrystalline boron suboxide (B_6O) material prepared by uniaxial hot-pressing are sparsely known. We recently reported on the nanoindentation profiles, nanoindentation hardness, and elastic modulus determined by using the Oliver-Pharr method. To complement our earlier reports on the analysis of the load-displacement indentation response of hot-pressed B_6O and for the first time, we present and discuss results giving an insight into the temporal evolution of the nanoindentation creep behaviour in B_6O ceramics.

Keywords: Boron suboxide, B_6O, nanoindentation, nanoindentation creep

* Corresponding Author

Office F7, Building 14F,
Materials Science and Manufacturing,
Council for Scientific and Industrial Research,
P.O. Box 395,
Pretoria 0001,
South Africa

Tel.: +27 12 841 3089, Fax.: +27 12 841 3378

Email: RMachaka@csir.co.za (Ronald Machaka)

1. Introduction

Boron suboxide (B_6O) is a boron-rich ceramic material. It is sometimes considered the third hardest material only after diamond and cBN [1]. The ceramic material is characterised by an α-rhombohedral boron-type structure [2] which is similar to that of α-B_{12} or boron carbide B_4C [3]. It exhibits a rather unusual and wide range of superior properties such as a low density, high mechanical strength, and high chemical inertness in addition to the super hardness. Furthermore, the material can be prepared at less extreme conditions of pressure and temperature as compared to diamond and cBN [1, 4].

Data concerning the investigation of the nano-mechanical properties of hot-pressed B_6O by nanoindentation did not exist in literature until recently [5, 6], in spite of the fact that the analysis of nano-mechanical properties is fast becoming an increasingly useful tool in a variety of scientific and engineering fields. Apparently, investigations into the nano-mechanical properties of hot-pressed B_6O by nanoindentation appear to have been neglected in favour of the improvement of densification and fracture toughness of the B_6O-based composites.

In brief, nanoindentation is now well established as a powerful means of characterizing the near-surface nano-mechanical properties (hardness, elastic modulus, and nanoindentation creep for example) of materials, see references [5–10] for example. The technique involves driving an indenter of known geometry into a specimen surface while simultaneously measuring the applied load-displacement (*P*-*h*) data. The measured unloading *P*-*h* data is typically analysed using the Oliver-Pharr method [8]. The conventional analysis of the *P*-*h* data usually yields the nanoindentation hardness and elastic modulus material properties [6–8].

We recently reported on the *P* - *h* response of hot-pressed B_6O measured during nanoindentation tests (see Figure 1 below, [6]). Jiao et al. have also independently reported on *P*-*h* response [5]. We further characterized the hardness and the elastic modulus in accordance with the Oliver-Pharr approach, and the related indentation size effects.

The typical instrumented indentation load-time profile is a trapezoidal loading function, where at maximum penetration depth the load is held constant prior to unloading. According to Mayo et al. [9], the relative change in the indenter displacement with time can be referred to as the nanoindentation creep of the specimen material. The constant load method is now one of the most popular approaches when analysing the creep properties of the material by nanoindentation [10].

The room temperature nanoindentation creep behaviour phenomenon has been observed and reported in some metals [11, 12], polymers [13], ceramics [14], and even in concrete [15] and wood [16].

However, this phenomenon has never been reported for B_6O or any other α-rhombohedral boron-type structured ceramic material for that matter.

The aim of this letter is two-fold. Firstly, it seeks to complement our earlier reports on the analysis of the load-displacement indentation response of hot-pressed B_6O, see reference [6]. Secondly, based on a quantitative analysis approach, the letter also seeks to present evidence of room-temperature nanoindentation creep behaviour observed in B_6O ceramics during short holding durations. The mechanisms at play during the temporal evolution of the nanoindentation creep behaviour in hot-pressed B_6O will be discussed.

2. Materials and experimental methods

B_6O powder used in this work was synthesized at the Fraunhofer Institute for Ceramic Technologies and Systems in Dresden, Germany as detailed by Andrews et al. in [17]. The prepared B_6O powder was uniaxially hot-pressed in hBN pots under argon environment at 1800 °C and 50 MPa for 20 min. The density of the compacts measured 2.44 g/cm^3. The uniaxially hot-pressed B_6O compacts were then metallographically prepared using a method prescribed by Machaka et al. in [18]. The character of the material has been reviewed [1, 6, 17, 18].

The nanoindentation measurements were performed using a CSM Instruments NHTX Nanohardness Tester at Nelson Mandela Metropolitan University in Port Elizabeth, South Africa. The indenter was fitted with a typical diamond Berkovich indenter tip. At least twelve separate indents were performed at different positions on the sample surface at room temperature. A maximum load of 100 mN, a loading rate of 200 mN/min, an indenter approach speed of 2000 nm/min, and a holding duration of about 17 s at the maximum load during which the load-displacement-time creep response data was recorded.

The maximum applied load, holding time, and loading rate used to assess the creep response of the material were all not varied in this study.

The topography of specimen surfaces and indentation impressions were examined using atomic force microscopy (AFM) also attached to the same instrument.

3. Results and discussions

3.1. Measured nanoindentation data

Figure 1 below depicts the representative *P-h* data for hot-pressed B_6O measured during nanoindentation tests with a Berkovich diamond indenter at room temperature.

The *P-h* response curves depicted are smooth with no evidence of pile-ups or sink-ins, an unloading 'nose', or unusual indentation artefacts. This is generally an indication of the absence of detectable phase transformations, surface cracking, or unloading too quickly – in the case of an unloading 'nose'.

The AFM topography scan around the indentation residual impression (over a scan size of 3.8 μm × 3.8 μm) is shown in Figure 2. The AFM topography scan also shows a fairly uniform surface topography with no visible evidence of indentation artefacts (such as pile-ups or sink-ins). The AFM profilometric data analysis was done using Gwyddion v2.24.

The specimen surface appears to be characterized with an average roughness (R_a) of about 7 nm with a root mean square surface roughness amplitude (R_q) of 9 nm. The surface roughness at the indentation site is a very small fraction of the maximum indentation depth and therefore, we suspect that it does not appear to influence the mechanical properties significantly.

3.2. Nanoindentation creep

In order to investigate creep parameters from simple nanoindentation measurements, data collected during the conventional nanoindentation test holding step, as illustrated in Figure 1b, was used. This approach is in accordance with the constant load method as first reported by Mayo et al. [9] and later by many others; see references [10, 13, 14], for example.

Figure 3 shows a typical creep displacement-time curve measured during the nanoindentation holding step. The indenter displacement into the sample during the constant peak load holding step is presented against the holding time. Data points depict experimental results while the solid line shows the fitted response according to an empirical Equation 1. Figure 3 shows a good agreement between fitted and experimental *h-t* data for the creep of B_6O during holding period at maximum load.

Based on the observations, the initial stage in Figure 3 is relatively brief and is characterized by transient creep with a rapidly decreasing creep strain rate due to the creep resistance of the material increasing by virtue of material deformation. The subsequent stage is characterized by steady state creep (i.e. a constant creep strain rate, $\dot{\varepsilon} \rightarrow 0$, in the case of B_6O) in which competing mechanisms of strain hardening and recovery may be present [19, Part B 3.3]. The evidence hints that the material is fully creep resistant. The existence of a tertiary creep region is not evident here.

3.3. Analysis of indentation creep data

The curve fitted to the experimental *h-t* data in Figure 3 follows an empirical law depicted in Equation 1 below:

$$h(t) = h_0 + a \cdot \ln(t - t_0) + k \cdot t \qquad (1)$$

where $h(t)$ is indenter displacement during the holding step, h_0, a, and k are best-fit parameters derived from the fitting protocol in Equation 1. The best-fit parameter t_0 is the time at which the creep process is started and is also derived from the fitting protocol.

According to Mayo and Nix [9], the creep strain rate $\dot{\varepsilon}$, is a function of depth and can be expressed as:

$$\dot{\varepsilon} = \frac{1}{h} \cdot \frac{dh}{dt} \qquad (2)$$

In this work, the creep strain rate data was deduced by first fitting the *h-t* creep curve during holding time with Equation 1 and then differentiating Equation 1 with respect to time (shown in Figure 3).

To characterize the nanoindentation creep in hot-pressed B_6O and its dominant mechanism, there exists an empirical relation between the creep strain rate and the stress. In the secondary or steady-state creep domain it can be simplified as Equation 3 shown below [11]:

$$\varepsilon = B \cdot \sigma^n \qquad (3a)$$

$$\ln(\dot{\varepsilon}) = \ln() + n \cdot \ln(\sigma) \qquad (3b)$$

where σ is the stress, B is a constant, and n is the stress exponent. The stress exponent is determined from the slope of the $ln(\dot{\varepsilon})$ versus $ln(\sigma)$ plot according to Equation 3b.

The actual stress field, σ beneath the indenter tip during test is however known to be complex; it varies from high levels in the vicinity of the tip to vanishingly small values in remote regions as predicted in the expanding cavity model [7]. In practice however, according to Goodall and Clyne [10], an average or effective form of this stress field is often handy, it can be expressed as Equation 4 below. In other terms, the effective stress is taken to be applied indentation load P, divided by the projected contact area [8].

$$\sigma = \frac{P}{24.56 \cdot h^2} \qquad (4)$$

The stress exponent n, is a parameter of key importance in this study since it is commonly used to give indications on the dominant creep mechanism. As is commonly known, see references [20, 21] for example; the diffusion creep mechanism is associated with $n \approx 1$, the grain boundary sliding creep

mechanism $1 < n < 2$, and when the $n > 3$, the dislocation movement is considered to be the dominant creep behaviour [22].

Figure 4 shows the log-log plot of $\dot{\varepsilon}$ versus σ for hot-pressed B_6O. The form of the plot resembles the logarithmic strain-rate versus stress plot in conventional tensile tests, and other researchers have observed the same [7, 10, 23]. The variation of the stress component with $ln(\sigma)$ has been determined and is also shown therein as an insert.

The values of n (see Figure 4 insert) differ at different points of the fitted strain rate-stress curve. The stress exponent decreased from about 0.96 on average at the start of the nanoindentation creep test (right hand side of plot) to about 0.14 on average towards the end of the test. This clearly indicates a change in the dominant creep mechanism.

The stress component at high stresses is closer to unity indicating that transient to early creep phenomena observed in B_6O are probably governed by a vacancy-diffusive mechanism. The stress component values at lower stresses rapidly tend to zero; indicating the slowing down of the vacancy-diffusive mechanism. Unfortunately, no known creep data for B_6O is available for comparison at the moment. However, an investigation on the creep of B_4C and α-AlB_{12} (materials having similar structure) was presented by Abzianidze et al. [21]. Based on their conclusions, creeping in the α-rhombohedral boron-type materials takes place via the vacancy-diffusive mechanism, for which $n = 1$.

The considerable degree of scatter in the steady-state creep stage (see ringed region in Figure 4 insert) has been attributed to two possible reasons. Firstly, the nanoindentation creep analysis method generates many stress strain data points from a single creep hold but can be sensitive to slight thermal fluctuations in the raw data [24]. Secondly, unlike conventional tests, the indentation depth is constantly changing and new material is continually entering the stress field and undergoing primary creep [24, 25]. However, although the nanoindentation creep behaviour is considerably more complex than that in conventional uniaxial tensile tests [26], it has since been established that the stress exponent evaluated using the indentation approach is expected to be in good agreement with those values obtained by conventional tensile tests [10, 12].

Overall, the results revealed that the material is creep resistant and the existence of a tertiary creep region is not evident here. Greater loads and higher temperature creep experiments at longer holding durations might be required to investigate this phenomenon further.

4. Summary and conclusions

Based on the quantitative and comprehensive analysis, the study also seeks to present evidence of room-temperature nanoindentation creep behaviour observed in B_6O ceramics during short holding durations.

From these results the stress component at high stresses is closer to unity indicating that transition to early creep phenomena observed in B_6O is probably governed by a vacancy-diffusive mechanism. The stress component values at lower stresses rapidly tend to zero indicating no creep at all. The transient and steady state creep stages were observed. The existence of a tertiary creep region is not evident here. The results revealed here hint that the material also has a superior creep resistant property.

Acknowledgements

We gratefully acknowledge the useful contributions of W. Goosen, M. Herrmann, K. Jakata, and J. Neethling and the generous financial support from the DST/NRF Centre of Excellence in Strong Materials and the University of the Witwatersrand Mellon Postgraduate Award.

References

[1] M. Herrmann, I. Sigalas, M. Thiele, M. Müller, H.-J. Kleebe, A. Michaelis, Boron suboxide ultrahard materials, Int. J. Refract. Met. Hard Mater. 39 (2013) 53-60.

[2] I. Higashi, M. Kobayashi, J. Bernhard, C. Brodhag, F. Thévenot, Crystal Structure of B_6O, in: D. Emin (Ed.), AIP Conference Proceedings: Boron-Rich Solids 231 (1991) 201-204.

[3] A. Suri, C. Subramanian, J. Sonber, T. C. Murthy, Synthesis and consolidation of boron carbide: a review, Int. Mater. Rev. 55 (2010) 4-40.

[4] C. Chen, D. He, Z. Kou, F. Peng, L. Yao, R. Yu, Y. Bi, B_6O-Based Composite to Rival Polycrystalline Cubic Boron Nitride, Adv. Mater. 19 (2007) 4288-4291.

[5] X. Jiao, H. Jin, F. Liu, Z. Ding, B. Yang, F. Lu, X. Zhao, X. Liu, Synthesis of boron suboxide (B_6O) with ball milled boron oxide (B_2O_3) under lower pressure and temperature, J. Solid State Chem. 183 (2010) 1697-1703.

[6] R. Machaka, T. Derry, I. Sigalas, Nanoindentation hardness of hot-pressed boron suboxide, Mater. Sci. Eng. A 528 (2011) 5778-5783.

[7] A.C. Fischer-Cripps, in A.C. Fischer-Cripps (Ed), Nanoindentation, Springer New York, 2011, pp. 39-75.

[8] W.C. Oliver, G.M. Pharr, Measurement of hardness and elastic modulus by instrumented indentation: Advances in understanding and refinements to methodology, J. Mater. Res. 19 (2004) 3-20.

[9] M. Mayo, R. Siegel, A. Narayanasamy, W. Nix, Mechanical properties of nanophase TiO_2 as determined by nanoindentation, J. Mater. Res. 5 (1990) 1073-1082.

[10] R. Goodall, T. Clyne, A critical appraisal of the extraction of creep parameters from nanoindentation data obtained at room temperature, Acta Materia. 54 (2006) 5489-5499.

[11] L. Shen, W.C.D. Cheong, Y.L. Foo, Z. Chen, Nanoindentation creep of tin and aluminium: A comparative study between constant load and constant strain rate methods, Mater. Sci. Eng. A 532 (2012) 505-510.

[12] R. Roumina, B. Raeisinia, R. Mahmudi, Room temperature indentation creep of cast Pb-Sb alloys, Scripta Mater. 51 (2004) 497-502.

[13] S. Yang, Y.-W. Zhang, K. Zeng, Analysis of nanoindentation creep for polymeric materials, J. Appl. Phys. 95 (2004) 3655-3666.

[14] M. Song, Y. Liu, X. He, H. Bei, W. Hu, F. Liu, Z. Li, Nanoindentation creep of ultrafine-grained Al_2O_3 particle reinforced copper composites, Mater. Sci. Eng. A 560 (2013) 80-85.

[15] C.A. Jones, Z.C. Grasley, Short-term creep of cement paste during nanoindentation, Cement Concrete Comp. 33 (2011) 12-18.

[16] W. Tze, S. Wang, T. Rials, G. Pharr, S. Kelley, Nanoindentation of wood cell walls: Continuous stiffness and hardness measurements, Compos. Appl. Sci. Manuf. 38 (2007) 945-953.

[17] A. Andrews, M. Herrmann, T. Shabalala, I. Sigalas, Liquid phase assisted hot pressing of boron suboxide-materials, J. Eur. Ceram. Soc. 28 (2008) 1613-1621.

[18] R. Machaka, T. Derry, I. Sigalas, M. Herrmann, Analysis of the indentation size effect in the microhardness measurements in B_6O, Adv.Mater. Sci. Eng. 2011 (2011) 539252.

[19] K.-H. Grote, E.K. Antonsson, Springer Handbook of Mechanical Engineering, Springer, 2009.

[20] W.R. Cannon, T.G. Langdon, Creep of ceramics, J. Mater. Sci. 18 (1983) 1-50.

[21] T. Abzianidze, A. Eristavi, S. Shalamberidze, Strength and Creep in Boron Carbide (B_4C) and Aluminum Dodecaboride (α-AlB_{12}), J. Solid State Chem. 154 (2000) 191-193.

[22] T. H. Courtney, Mechanical Behavior of Materials, McGraw Hill Education (Asia), 2004.

[23] W. Yin, S. Whang, R. Mirshams, C. Xiao, Creep behavior of nanocrystalline nickel at 290 and 373 K, Mater. Sci. Eng. A 301 (2001) 18-22.

[24] M. I. Davies, High temperature nanoindentation characterisation of P91 and P92 steel, Ph.D. Thesis, University of Nottingham, 2013.

[25] J. Dean, A. Bradbury, G. Aldrich-Smith, T. Clyne, A procedure for extracting primary and secondary creep parameters from nanoindentation data, Mech. Mater. 65 (2013) 124-134.

[26] X. Zhu, X. Liu, F. Zeng, F. Pan, Room temperature nanoindentation creep of nanoscale Ag/Fe multilayers, Mater. Lett. 64 (2010) 53-56.

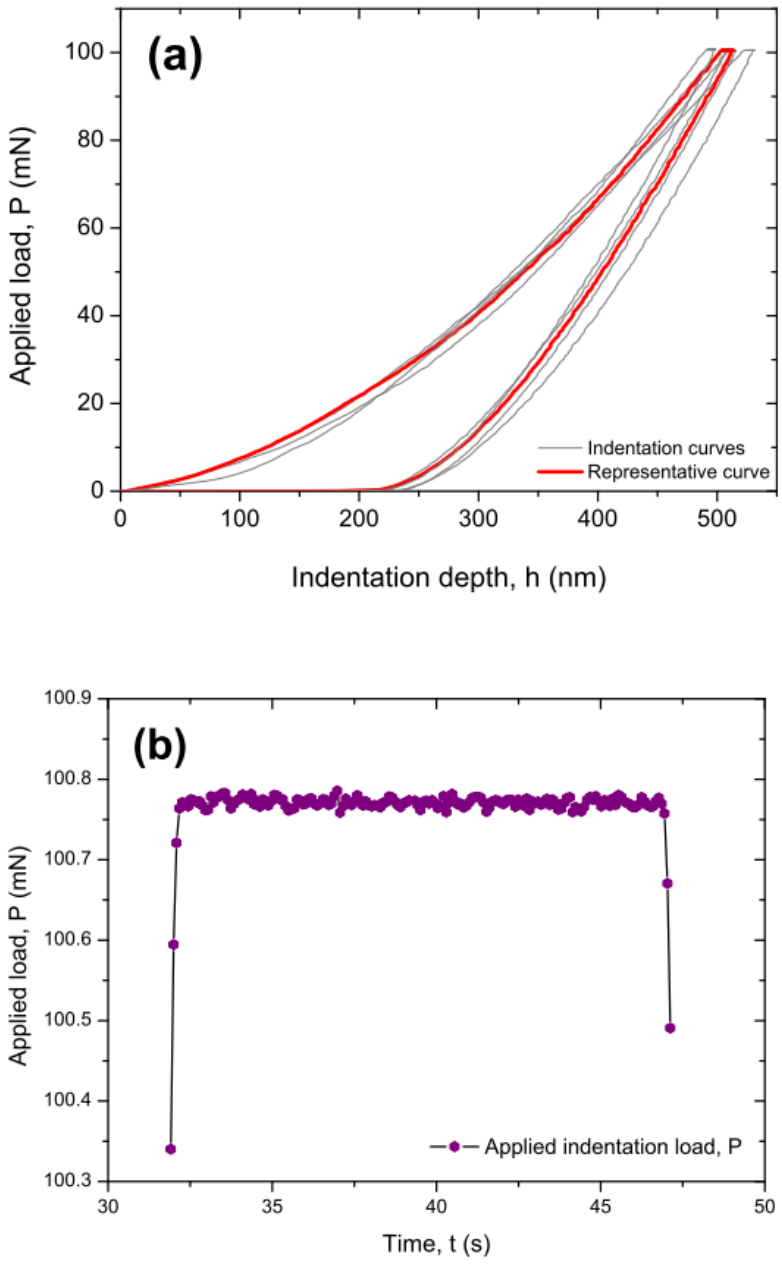

Figure 1:

The typical nanoindentation *P-h* response measured from hot-pressed B_6O samples (a). A *P-t* curve showing the typical peak-load hold segment of nanoindentation experiments (b).

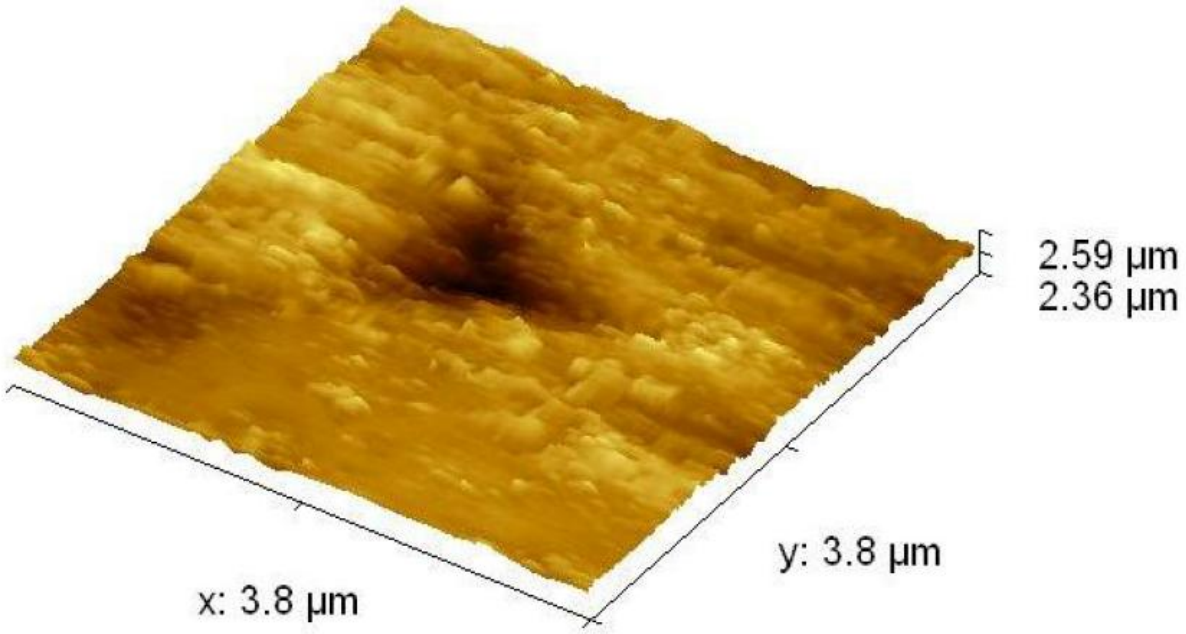

Figure 2:

An AFM image measured on an indented site [6]. The profilometric data analysis was done using Gwyddion v2.24.

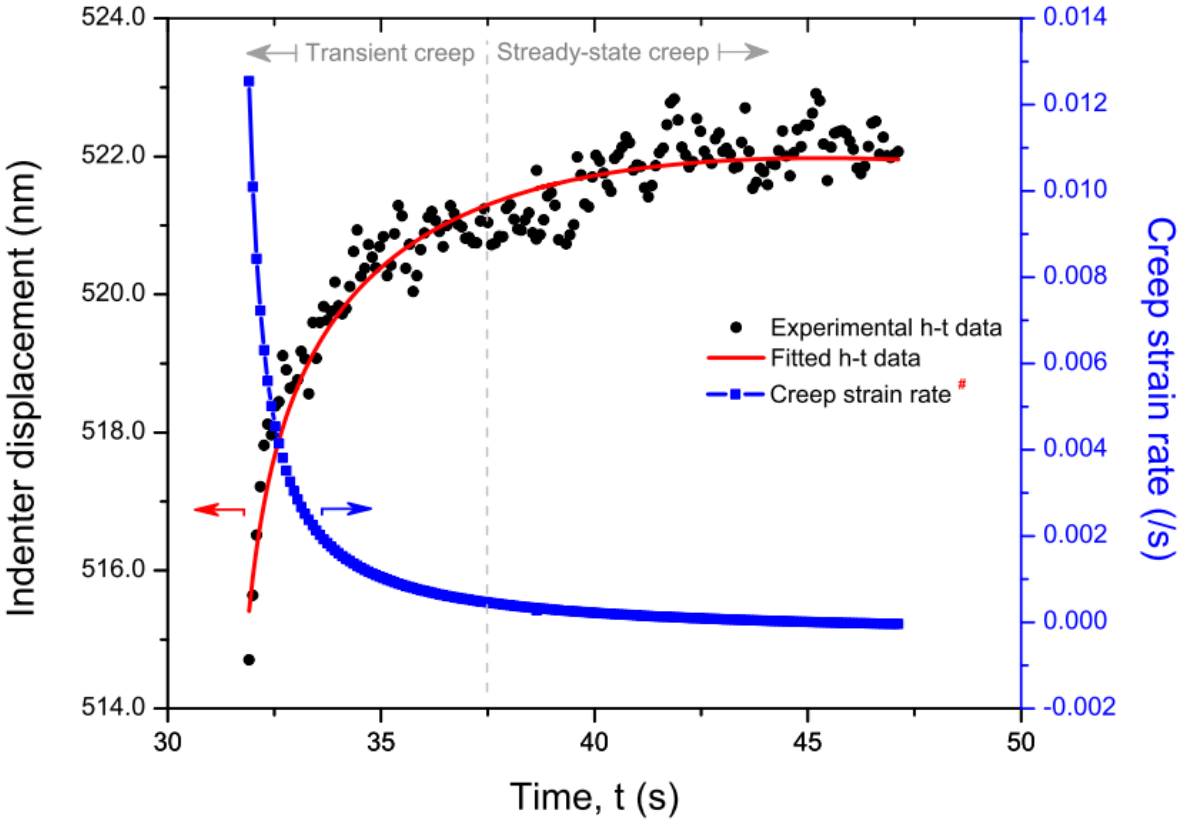

Figure 3:

A typical creep displacement-time curve during the nanoindentation creep of hot-pressed B_6O at room temperature. The transient and steady-state creep stages are shown based on the fitted creep strain rate curve.

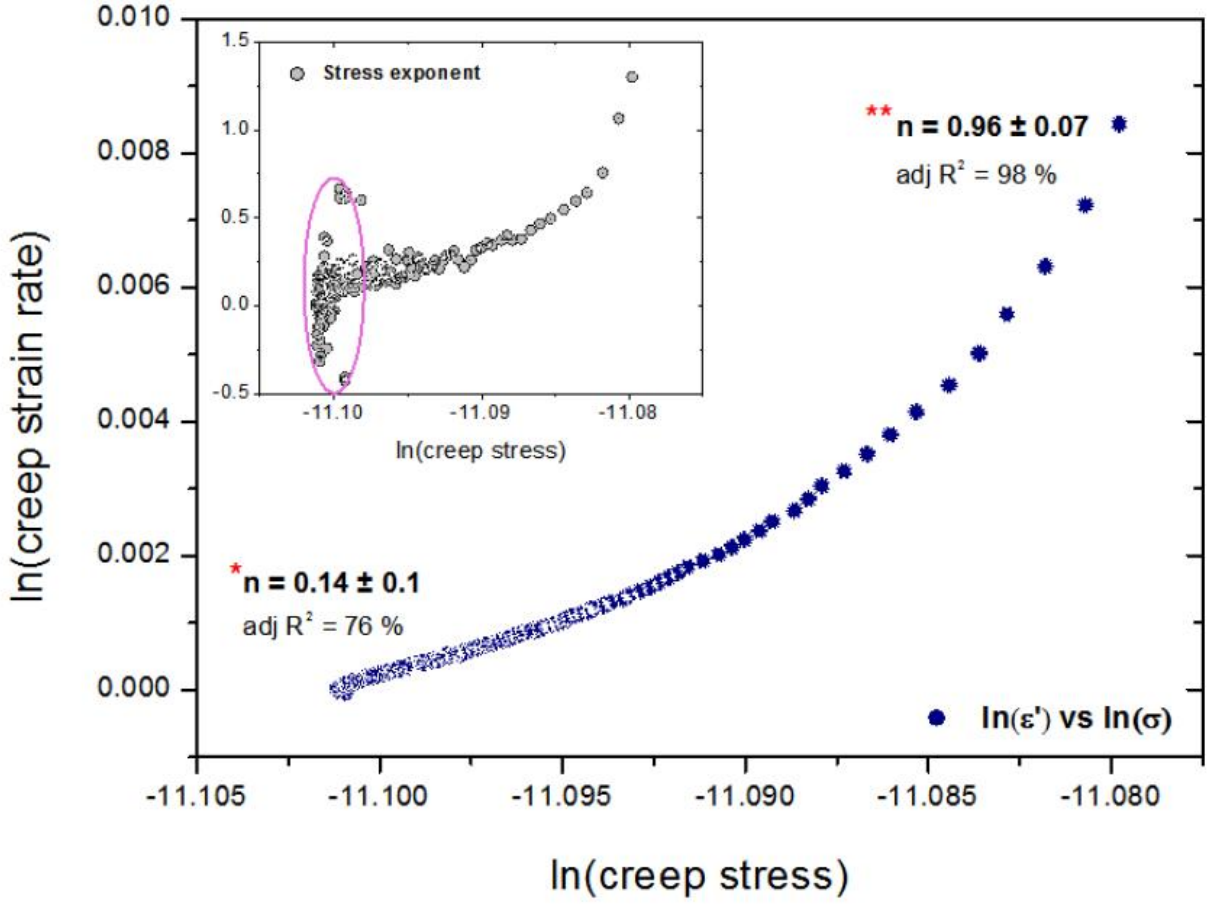

Figure 4:

The bi-logarithmic plot of the creep strain rate versus the effective stress obtained from the data in Figure 3. The insert shows the variation of stress component, *n* plotted as a function of *ln*(σ).